Deterministic role of salinity advection feedback in the multi-centennial variability of AMOC revealed in an EC-Earth simulation

Ning Cao[1,2,3], Qiong Zhang[2,3*], Katherine Elizabeth Power[2,3], Frederik Schenk[3,4], Klaus Wyser[3,5], and Haijun Yang[6,7]

[1]College of Ocean and Meteorology and CMA-GDOU Joint Laboratory for Marine Meteorology, Guangdong Ocean University, Zhanjiang, 524088, China

[2]Department of Physical Geography, Stockholm University, Stockholm, 10691, Sweden

[3]Bolin Centre for Climate Research, Stockholm University, Stockholm, 10691, Sweden

[4]Department of Geological Sciences, Stockholm University, Stockholm, 10691, Sweden

[5]Swedish Meteorological and Hydrological Institute (SMHI), Norrköping, 60176, Sweden

[6]Department of Atmospheric and Oceanic Sciences and Institute of Atmospheric Science and CMA-FDU Joint Laboratory of Marine Meteorology, Fudan University, Shanghai, 200438, China

[7]Shanghai Scientific Frontier Base for Ocean-Atmosphere Interaction Studies, Fudan University, Shanghai, 200438, China

[*]Corresponding author: Qiong Zhang (qiong.zhang@natgeo.su.se)

Key Points:

- Multi-centennial variability with a spectrum peak at approximately 200 years in a pre-industrial control simulation using EC-Earth3
- The positive salinity advection feedback by the perturbation flow of mean salinity gradients is essential to sustain such an oscillation
- Mean advection of salinity anomalies and the vertical mixing or convection cause a negative feedback to restrain the AMOC anomalies

Abstract

Significant multi-centennial climate variability with a clear peak at approximately 200 years is found in a pre-industrial control simulation conducted with the EC-Earth3 climate model. The oscillation mainly emerges from the North Atlantic and appears to be closely associated with the Atlantic Meridional Overturning Circulation (AMOC). By examining the salinity advection feedback, we find that the perturbation flow of mean subtropical-subpolar salinity gradients in the subpolar area governs as positive feedback to the AMOC anomaly. Meanwhile, the mean advection of salinity anomalies and the vertical mixing or convection acts as negative feedback to restrain the AMOC anomaly. In a warmer climate, although the AMOC becomes weaker, such low-frequency variability still exists, indicating the robustness of the salinity advection feedback mechanism.

Plain Language Summary

On timescales longer than 100 years, the identification of climate variability facts and driving mechanisms remains elusive due to lacking observations. Paleoclimatic reconstructions from proxy records show multi-centennial variability in the climate system. Such low-frequency climate variabilities are also found in simulations using fully coupled climate models. Previous modeling studies suggested that such oscillations are driven by salinity anomalies coming from the South Atlantic or the Arctic, which cannot explain the continuous energy source that sustains such a long period of oscillation. Here we use a 2000-years long simulation conducted with a climate model EC-Earth3 under pre-industrial forcing conditions to investigate the origin of the multi-centennial climate variability. Our results confirmed a deterministic role of the salinity advection feedback in the subtropical-subpolar North Atlantic in modulating the AMOC variability at multi-centennial time scale. In the ongoing global warming, even though the AMOC is weakening, the multi-centennial oscillation still maintains.

1 Introduction

Multi-decadal to multi-centennial variabilities in climate system have been observed in paleoclimate proxy records (*Delworth and Mann,* 2000*; Sicre et al.,* 2008*; Jones et al.,* 2009*; Mann et al.,* 2009*; Menary et al.* 2012*; Srokosz and Bryden* 2015*; Ayache et al.* 2018*; Thirumalai et al.* 2018) and long climate model simulations (*Vellinga and Wu* 2004*; Park and Latif* 2008*; Friedrich et al.* 2010*; Menary et al.* 2012*; Delworth and Zeng* 2012*; Jiang et al.* 2021). *Askjær et al.* (2022) analyzed 120 temperature reconstructions during the Holocene and examined transient Holocene simulations from 9 models. Significant multi-centennial variability was found to be centered in the frequency band >100 to <250 years in both proxies and models.

In proxy records, climate variability can arise from both internal processes (*Mann et al.* 2014*; Zhang et al.* 2019) and external forcing changes (e.g., solar irradiance and volcanic eruptions, see *Ottera et al.* 2010*; Mann et al.* 2021). These are difficult to distinguish from each another. In climate models, however, as the input can be manually controlled, it is possible to solely investigate internal variability without external forcing changes using control simulations. Many studies attribute such low-frequency climate variabilities to the North Atlantic Meridional Overturning Circulation (AMOC), a phenomenon responsible for transporting ocean heat northward through the Atlantic Ocean (*Delworth and Zeng* 2012*; Lapointe et al.,* 2020*; Dima et al.,* 2022).

Several studies have reported the presence of multi-centennial climate variability in their model, e.g., KCM model (*Park and Latif* 2008), LOVECLIM model (*Friedrich et al.* 2010), GFDL CM2.1 model (*Delworth and Zeng* 2012), IPSL-CM6A-LR model (*Boucher et al.* 2020; *Jiang et al.,* 2021), EC-Earth3 model (*Meccia et al.* 2022). Many of these studies attribute the multi-centennial climate variability to seawater density fluctuations over regions of deep water formation in the North Atlantic, which are considered to be induced by salinity anomalies. Several different mechanisms have been proposed to explain where these salinity anomalies originate from. *Park and Latif* (2008) emphasized the importance of transporting freshwater anomalies advected from the South Atlantic and transported northward alongside AMOC, a mechanism also supported by *Delworth and Zeng* (2012). On a decadal scale, the Agulhas leakage from the Indian Ocean into the South Atlantic might contribute to the AMOC variability with the same order of magnitude as northern sources (*Biastoch et al. 2008*) but longer timescales are more difficult to study. Based on the HadCM3 control simulation, previous studies reported multi-decadal to centennial variability of the AMOC, which was considered to be strongly related to salinity anomalies in the deep-water formation regions arriving via two pathways: from a coupled feedback in the equatorial Atlantic Ocean (*Vellinga and Wu* 2004) and from variability in the Arctic Ocean, possibly driven by stochastic sea level pressure (*Jackson and Vellinga* 2013). Some studies argue that salinity anomalies coming from the Arctic Ocean are dominated by freshwater exchanges between the Arctic and North Atlantic regions (*Jungclaus et al.* 2005; *Hawkins and Sutton* 2007*; Pardaens et al.* 2008*; Jahn and Holland* 2013*; Jiang et al.* 2021*; Meccia et al.* 2022). These diagnosed studies provide different views that partly explain the fluctuations of AMOC on different timescales. However, the main difficulty lies in the continuous energy source that sustains such a long period of oscillation. The Arctic salinity anomalies act at a similar pace to AMOC but can hardly be considered as the energy source that drives the AMOC fluctuations.

Very recently, using simple conceptual models, *Li and Yang* (2022) (LY22, hereafter) identified a self-sustained multi-centennial mode in the AMOC. Their work provides a more fundamental theory of such low-frequency variability. In the present work, we use a 2000-year output from a control experiment conducted with the EC-Earth3 climate model to examine the multi-centennial climate variability. We provide robust proof of the theory by LY22 and demonstrate the physical process of how the multi-centennial oscillation could sustain itself in our simulation.

2 Model Description and Experimental Design

EC-Earth is a fully coupled Earth system model that integrates several state-of-the-art components in the climate system, including atmosphere, ocean, sea ice, land, and biosphere. It is developed by the European consortium of more than 30 research institutions and is widely used in various studies on climate change simulations, climate predictions, sensitivity studies, and process studies (*Semedo et al*. 2016; *Wyser et al*. 2020a,b; *Zhang et al*., 2021; *Myriokefalitakis et al*. 2022). We use the CMIP6 version of EC-Earth with EC-Earth3-LR configuration, coupling the atmosphere, land, ocean and sea-ice components. LR stands for low resolution for the atmospheric model. The atmospheric part is the Integrated Forecasting System (IFS) model, with cycle 36r4 (TL159, linearly reduced Gaussian grid equivalent to 320 × 160 longitude/latitude; 62 levels; top level 5 hPa). The ocean component is the Nucleus for the European Modelling of the Ocean version 3.6 (NEMO3.6) (ORCA1 tripolar primarily 1 degree with meridional refinement down to 1/3 degree in the tropics; 362 × 292 longitude/latitude; 75 levels; top grid cell 0-1 m). NEMO includes the Louvain-la-Neuve Sea-ice model version 3 (LIM3), a dynamic thermodynamic sea-ice model with five ice thickness categories. The latest model development is described in detail by *Döscher et al.* (2022).

We conducted a control simulation using the EC-Earth3-LR model under pre-industrial forcings. The atmosphere components are held constant at 1850 conditions. The simulation is initialized by a pre-run steady restart file (the output of approximately 500-year pre-industrial control simulation) and is integrated for 2000 years. To investigate the sensitivity of multi-centennial climate variability to global warming, we also conducted two experiments by changing the CO_2 concentration to 400 ppm (E400) and 560 ppm (E560) at the same start year as the E280 experiment (E280), which are integrated for more than 3000 years. The last 2000-year outputs of the three simulations are used in this work.

3 Results and the Driving Mechanism

The time series of global mean surface air temperature (Figure 1a) shows significant multi-centennial variability with a distinct peak at approximately 200 years. This low-frequency signal is most pronounced in the northern hemisphere, especially in the North Atlantic. The variation of meridional ocean heat transport across 40°N in the Atlantic is highly consistent with the global mean surface air temperature (Figure 1b), which was considered to trigger the temperature changes in the North Atlantic and the Arctic, and even in the entire Nothern Hemisphere (*Delworth and Zeng* 2012). It implies that the AMOC drives the northward ocean heat transport, which is in line with the previous suggestions the AMOC mainly drives the low-frequency variabilities in the Earth's climate system (*Delworth and Zeng,* 2012*; Lapointe et al.,* 2020*; Dima et al.,* 2022). We define the AMOC index as the annual-mean maximum ocean overturning stream function between 20°N to 70°N from depths 200 to 3000 meters. Figure 1c shows the time series of the AMOC index. The average strength of AMOC is 17.5 ± 1.3 Sv (1 Sv = 10^6 m^3 s^{-1}). The variation of the AMOC is highly correlated with the global mean surface air temperature.

The AMOC variation is mainly driven by density fluctuation over regions of North Atlantic Deep-Water (NADW) formation (*Danabasoglu* 2008*; Delworth and Zeng* 2012*; Dima et al.* 2022*)*, and this result can also be seen in our simulation (see Figure S1 in the supplement material). Seawater density depends on temperature and salinity, and in the NADW region, the salinity variation dominates the overall density fluctuation in these regions (see Figure S2). Here we define the NADW formation region as a horizontal ocean region between 70^{o}W - 10^{o}E and 50^{o}N - 80^{o}N, encompassing the Labrador Sea, Irminger Sea, and Greenland-Icelandic-Norwegian (GIN) Seas, which is referred to as the subpolar area in this work. In our simulation, the sea surface temperature (Figure 1d) and sea surface salinity (Figure 1e) averaged over the subpolar area show similar variations as those of the AMOC index. In addition, spectrum analyses of these time series show similar spectra with a distinct peak around 200 years (Figure 1f).

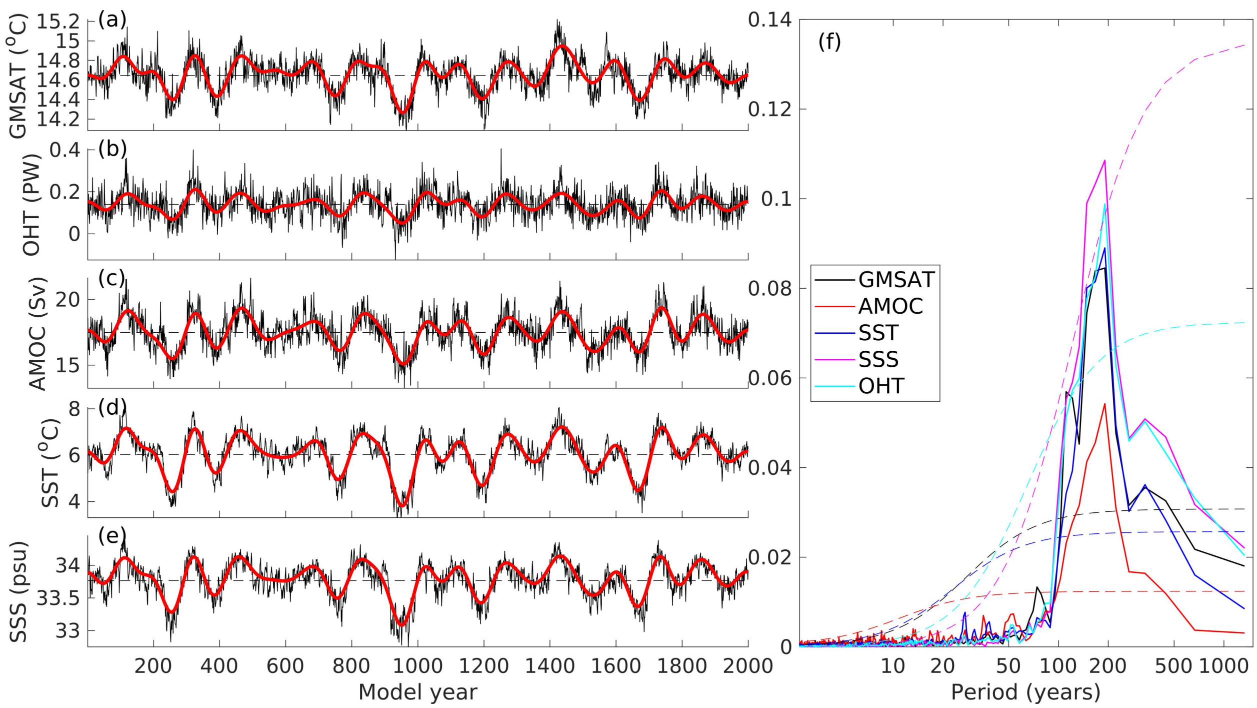

Figure 1. (a~e) Time series of global mean surface air temperature (GMSAT), ocean heat transport crossing the 40^{o}N in Atlantic (OHT, 1 PW = 10^{15} Watt), AMOC index, sea surface temperature (SST) and sea surface salinity (SSS) averaged over the subpolar area, together with the low-pass filtered series (red curves, using Lanczos method with 201 weights and a cutoff period of 100 years); (f) The power spectrums of these corresponding time series.

To investigate the origin of salinity anomalies in the subpolar area, Figure 2 shows the Hovmöller diagrams of the regressed zonal-integral salinity averaged at ocean layers of 0-100, 100-300, 300-500, 500-1000, 1000-2000 and 2000-3000 m across the Atlantic and Arctic basins, onto the low-pass-filtered AMOC time series. At the surface layer (0-100 m, Figure 2a), salinity anomalies are most pronounced in the subpolar area. No significant salinity anomalies are coming from the South Atlantic to the mid-latitude Atlantic, in contrast to that shown in *Delworth and Zeng* (2012). At the subsurface layer (100-300 m, Figure 2b), the anomalies in the subpolar area are much weaker than the surface layer, and a stable link between the subpolar and subtropical regions is established within about 100 years. The anomalies in the subtropical region become more robust at the 300-500 m layer (Figure 2c). At layers deeper than 500 m (Figure 2d~f), a southward advection of lagged salinity anomalies emerges clearly, as a result of strong convection in the subpolar area and the related southward flow to the lower branch of the AMOC. The upper layer salinity anomalies in the subpolar area are locally driven and may also be related to local salinity change in the subpolar Atlantic and Arctic. The accumulated anomalies at the upper layer subpolar ocean can sink and propagate southward with the help of the mean AMOC, reaching as deep as 3000 m in the North Atlantic (Figure 2f). This process can be seen clearly in Figure 3.

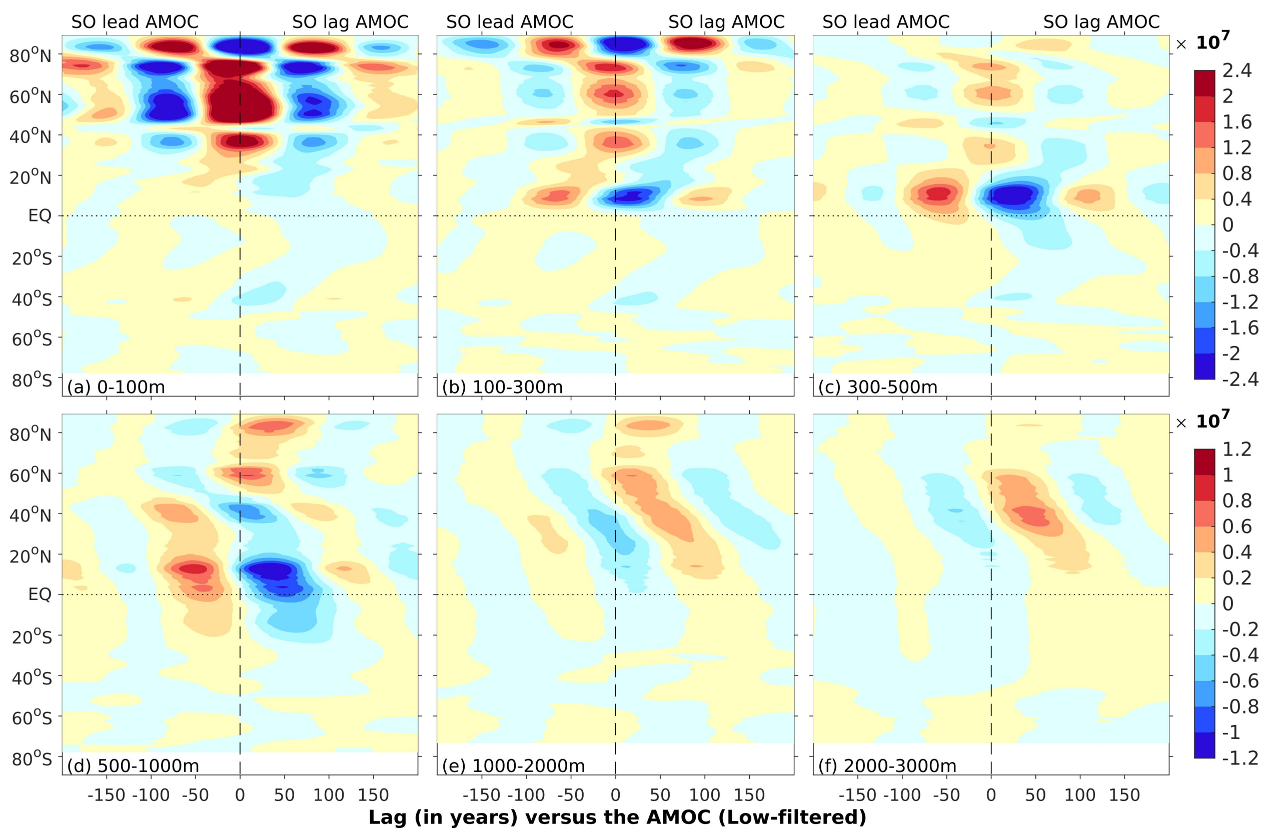

Figure 2. The zonal integral of the regression coefficients of salinity across the Atlantic basin versus the low-pass-filtered AMOC time series. Units are psu m Sv^{-1}. The y-axis is latitude, and the x-axis is lag to the time of maximum AMOC. Negative (positive) values on the time axis indicate periods leading (lagging) to the maximum AMOC. (a-f) Mean values at layers of 0-100, 100-300, 300-500, 500-1000, 1000-2000, and 2000-3000 m, respectively.

Figure 3 shows the latitude-depth profiles of zonally integrated salinity across the Atlantic and Arctic basins regressed on the AMOC time series when the time lags/leads the AMOC maximum by 80 to 100 years, with an interval of 20 years. An entire cycle of salinity variability evolution with a period of about 200 years can be seen consistent with Fig. 2f. From 80 to 60 years prior to the AMOC maximum, the negative salinity anomalies occupy the entire subpolar North Atlantic from surface to deep ocean and are most pronounced at the upper-500m layer, while positive anomalies can be seen in the subsurface layer of the subtropical North Atlantic. Negative anomalies in the subpolar area sink deep into the ocean, causing the surface anomalies to decrease. Meanwhile, positive anomalies in the subtropical region become stronger and broader. At 40 years prior, anomalies in the upper layer of the subpolar area have changed phases from negative to positive. The negative anomalies move southward at the deep ocean. Afterwards, positive anomalies in the subpolar area grow quickly, while negative anomalies occupy the deep ocean in the subtropical North Atlantic. At lag 0, when the AMOC reaches its maximum, positive salinity anomalies fill up the entire subpolar area, and apparent vertical mixing can be seen at about 60°N. The negative anomalies in the lower ocean of the subtropics move upward with enhanced amplitudes and connect with the anomalous negative salinity centered at about 10°N with a depth of approximately 300 m. Then, in the following 40 years, the subpolar area shows the distinct sinking of positive anomalies into the deep ocean, weakening the surface anomalies. The negative anomalies in the subtropical region are strengthening. At lag 40, most subpolar positive anomalies have sunk into the deep ocean and moved southward, and the negative anomalies in the subtropical region continue to strengthen and expand. At lag 60, the subpolar upper layer salinity anomalies change signs from positive to negative, while the sinking positive anomalies in the deep ocean keep moving southward. Afterwards, negative anomalies in the upper subpolar ocean continue to strengthen, as well as the positive anomalies in the subsurface layer of the subtropical region. At lag 100, the apparent sinking of negative anomalies in the subpolar area can be seen, with a similar pattern to lag -80, indicating the oscillation entering a new cycle.

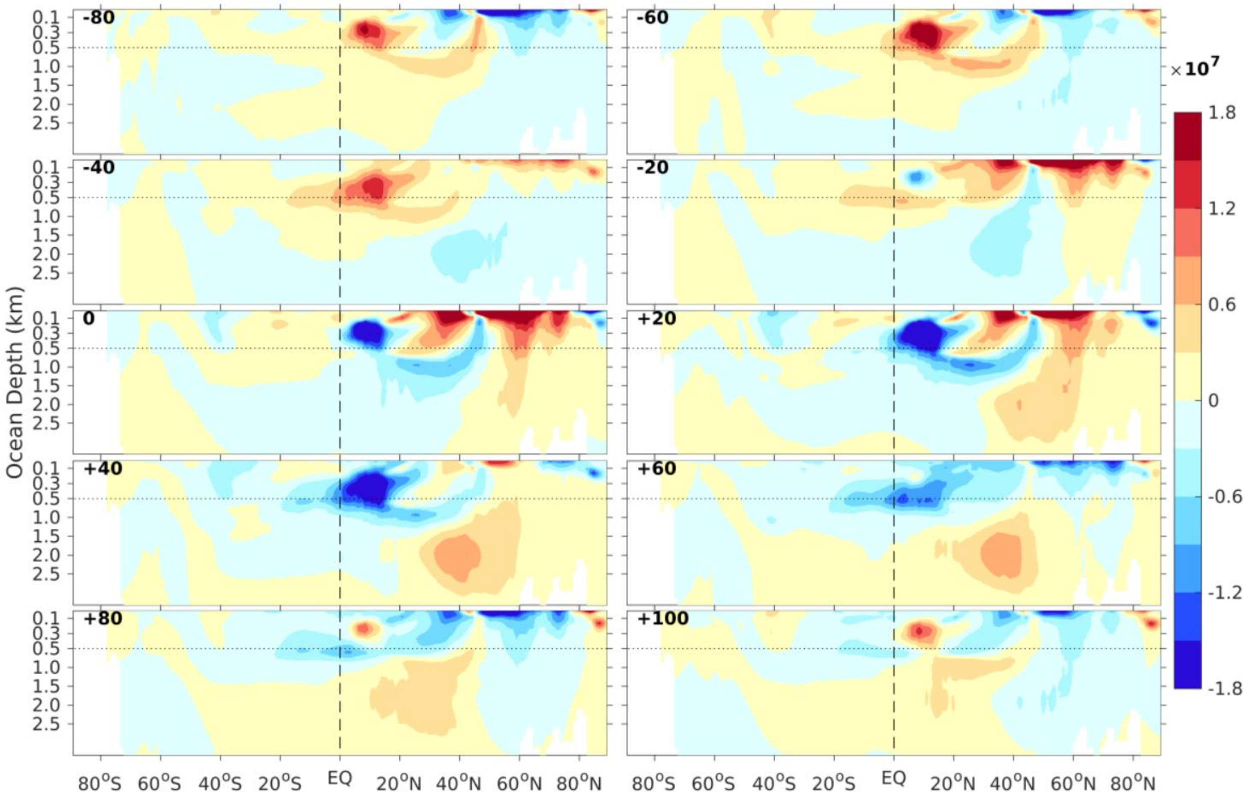

Figure 3. Latitude-depth profiles of zonal integral salinity across the Atlantic and Arctic basins regressed on the 100-year low-filtered AMOC time series. The lag is positive when the AMOC leads. Units are psu m Sv^{-1}. The scale of layers shallower than 500 m is amplified by two.

Figures 2 and 3 show that the surface salinity anomaly in the subpolar area is more locally developed rather than being transported from lower latitudes or the Arctic. We find that this local salinity anomaly (Figure 2a-b) is caused by the effect of perturbation advection of mean salinity. While the lower ocean salinity change (Figures 2e-f) is due to the effect of mean advection of salinity anomalies. The perturbation salinity advection effect is local, acting as positive feedback to incite the strong local signal in the upper ocean (Figure 2a-b). On the other hand, the mean salinity advection effect can be seen as a remote effect, causing a southward propagating signal in the lower ocean (Figures 2e-f) and acting as negative feedback to remove the anomalies out of the subpolar ocean. Our results confirm the theory in LY22's study that the perturbation salinity feedback provides the energy source for maintaining the oscillation while the mean salinity feedback dampens the salinity anomalies. In LY22, an enhanced mixing process in the subpolar ocean is also considered as a critical mechanism to weaken the positive salinity advection feedback and limit the oscillation amplitude. In Figure 3, this vertical mixing of salinity anomalies can be seen at the subpolar North Atlantic area latitudes.

We applied the small-perturbation theory to the salinity equation to quantify these effects and ignored the nonlinear advection terms. The anomalous meridional salinity advection is divided into the perturbation advection of mean salinity gradients and the mean advection of salinity anomaly. We define four boxes in the North Atlantic as follows: Box-1: the subtropical upper layer box, from 0° to 40°N across the Atlantic basin, vertically 0-300 meters; Box-2: the subpolar upper layer box, from 70°W to 10°E and from 50°N to 80°N, vertically 0-300 meters; Box-3: the subpolar deep layer box, from 70°W to 10°E and 50°N to 80°N, vertically 1000-3000 meters; Box-4: the subtropical deep layer box; from 0° to 40°N and between 1000 and 3000 meters. The variations of seawater salinity in Box-2 can be determined by the following equation as suggested in LY22 (Eq. 8a).

$$V_2\dot{S}_2' = q'(\overline{S_1} - \overline{S_2}) + \bar{q}(S_1' - S_2') - k_m(S_2' - S_3') \quad \text{(Eq-1)}$$

where V_2 is the volume of Box-2, q is the volume transport by the AMOC which can be divided into a mean state $\bar{q}$ and a perturbation q', S_i' is the perturbation salinity of each ocean box, $\overline{S}_i$ is the mean salinity during the reference period. Following LY22, we similarly define the enhanced mixing effect coefficient $k_m = \kappa(q')^2$ in which $\kappa = 1.0$ m^{-3} s (Note that the value of κ only affects the amplitude of the oscillation but not the period).

Figure 4 shows the lead-lag regression of terms that contribute to the salinity anomaly in Box-2 (S_2'). It is evident that the perturbation flow of mean salinity gradients from Box-1 to Box-2 (black curve) tends to have the same sign as S_2', indicating positive feedback to make S_2' grow. The mean advection of salinity anomalies (red curve) acts against S_2' , indicating a significant negative effect on the salinity change that drives the oscillation to change phase. The vertical mixing between Box-2 and Box-3 (blue curve) also acts as a negative feedback to limit S_2' . The most pronounced southward flow relating to the lower branch of the AMOC lags the maximum AMOC by about 40-50 years, so it acts as a lagged indirect negative feedback (cyan curve), helping to limit the S_2' by removing the mixed anomalies in Box-3 into Box-4. These results reveal that the multi-centennial variability of AMOC in our model is maintained by the positive feedback of the perturbation advection of mean salinity gradients, the negative feedback of the mean advection of salinity anomalies, as well as the enhanced vertical mixing in the subpolar ocean, which are in good agreement with the theoretical prediction of LY22.

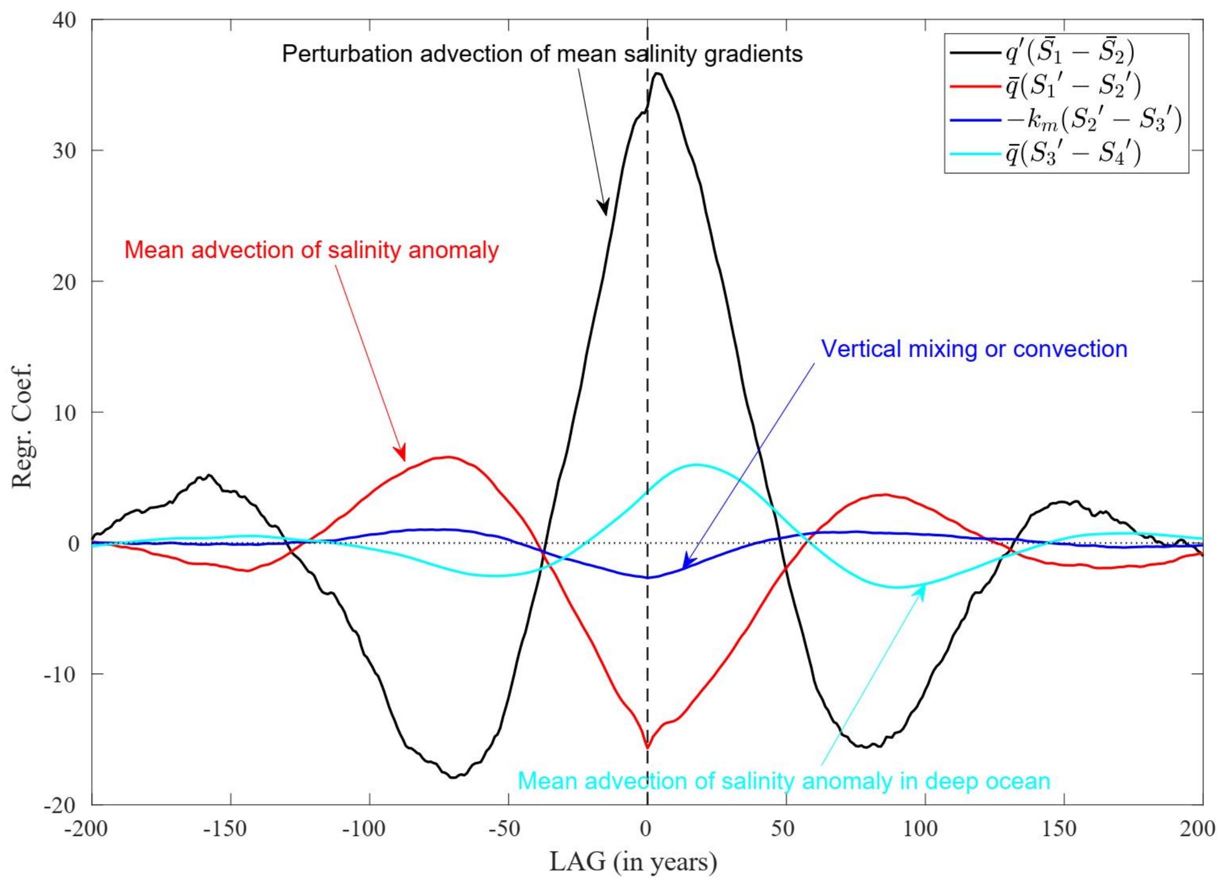

Figure 4. Regression of three direct terms (black, red and blue curves) contributing to variations of seawater salinity in Box-2 defined in Eq-1, and one indirect term (cyan curve) indicating the southward flow that is related to the lower branch of the AMOC, onto the time series of salinity in the Box-2.

4 Summary and Discussion

Using a 2000-year pre-industrial control simulation by the EC-Earth3-LR climate model, we identified a multi-centennial climate variability with a timescale of about 200 years. The global mean surface air temperature shows distinct multi-centennial climate variability, which can be attributed to the fluctuations of AMOC. A strengthened AMOC is associated with positive density anomalies over the deep-water formation region in the North Atlantic, and salinity variations dominate the overall density fluctuations in the subpolar area of the North Atlantic.

The mechanism to maintain the multi-centennial variability in the simulated climate system is disclosed in this work. The perturbation advection of the mean subtropics-subpolar salinity gradients causes positive feedback to the growth of the AMOC anomalies. Meanwhile, the mean advection of salinity anomalies and the vertical mixing or convection acts as negative feedback to restrain the AMOC anomalies. Both our fully coupled model simulation and simple conceptual model study of LY22 support that the subpolar salinity anomalies are mainly locally driven by the perturbed ocean circulation on the timescale of multi-centennial, not by the mean flow of salinity anomaly from the south Atlantic (*Delworth and Zeng* 2012) or the Arctic (*Jiang et al.* 2021*; Meccia et al.* 2022). Only by introducing the salinity advection feedback mechanism we can fully explain how the AMOC develops such a self-sustained oscillation.

The freshwater anomaly from the Arctic does have an impact on the seawater density in the subpolar area, but it cannot be considered as the energy source of AMOC fluctuations. In a warmer climate, such as the situation in ongoing global warming, the AMOC becomes weaker than it was in the pre-industrial period (*Rahmstorf et al*. 2015; *Caesar et al*. 2021), although there is a robust debate over the role of climate change versus the circulation's century-to-millennial-scale variability (*Kilbourne et al*. 2022; *Latif et al*. 2022). In our simulations under 400 ppm and 560 ppm CO2 forcing, the AMOC weakens (Figure S3a~c). However, the spectrums still capture the multi-centennial variability with the dominant oscillation periods around 100-300 years, as illustrated in Fig S3d. The oscillation amplitude is suppressed under higher CO_2 forcing. Similar results can be seen in *Meccia et al*. (2022). It further confirms that the multi-centennial oscillation of AMOC is an intrinsic mode in the system. Thus, a warmer climate has the potential to suppress the oscillation amplitude and to modify the oscillation periods through increases in ocean heat content, elevated freshwater flows from the melting ice sheets, and the shrinking of Arctic sea-ice, which deserves further study.

Data Availability Statement

The model simulated data to produce the main figures in this paper can be found at: https://doi.org/10.5281/zenodo.7304486 (a dataset of *Zhang et al.* 2022).

Acknowledgments

This research was supported by the Swedish Research Council (Vetenskapsrådet, grant no. 2022-03129 and 2017-04232). Ning Cao is supported by the National Natural Science Foundation of China (42130605, 42075036, and 41875071), the program for scientific research start-up funds of Guangdong Ocean University (R17056), and the State Scholarship Fund of China Scholarship Council (201908440188). Haijun Yang is supported by the National Natural Science Foundation of China (42230403). Frederik Schenk is funded by the Swedish Research Council for Sustainable Development (FORMAS 2020-01000). The simulations with EC-Earth3-LR and data analysis were performed using the ECMWF's computing and archive facilities and Swedish National Infrastructure for Computing (SNIC) at the National Supercomputer Centre (NSC), partially funded by the Swedish Research Council through grant agreement no. 2018-05973.

References

Askjær T. G., Zhang Q., Schenk F., et al. (2022), Multi-centennial Holocene Climate Variability in Proxy Records and Transient Model Simulations. *Quaternary Science Reviews*, *296*, 107801.

Ayache, M., Swingedouw, D., Mary, Y., et al. (2018), Multi-centennial variability of the AMOC over the Holocene: A new reconstruction based on multiple proxy-derived SST records. *Global and Planetary Change*, *170*, 172–189. doi: 10.1016/j.gloplacha.2018.08.016

Boucher, O., Servonnat, J., Albright, A. L., et al. (2020), Presentation and evaluation of the IPSL-CM6A-LR climate model. *Journal of Advances in Modeling Earth Systems*, *12*, e2019MS002010. doi:10.1029/2019MS002010

Buckley, M. W., Marshall, J. (2016), Observations, inferences, and mechanisms of the Atlantic Meridional Overturning Circulation: A review. *Reviews of Geophysics*, *54*(1): 5–63. doi:10.1002/2015RG000493.

Caesar, L., McCarthy, G.D., Thornalley, D.J.R. et al. (2021), Current Atlantic Meridional Overturning Circulation weakest in last millennium. *Nature Geoscience*, *14*, 118–120. doi:10.1038/s41561-021-00699-z

Danabasoglu, G. (2008), On multidecadal variability of the Atlantic meridional overturning circulation in the Community Climate System Model Version 3, *Journal of Climate*, *21*, 5524–5544. doi:10.1175/2008JCLI2019.1.

Delworth, T. L., & Mann, M. E. (2000), Observed and simulated multidecadal variability in the Northern Hemisphere. *Climate Dynamics*, *16*, 661–676. doi:10.1007/s003820000075

Delworth, T. L., & Zeng, F. (2012), Multicentennial variability of the Atlantic meridional overturning circulation and its climatic influence in a 4000-year simulation of the GFDL CM2.1 climate model. *Geophysical Research Letters*, *39*(13), L13702. doi: 10.1029/2012GL052107

Dima, M., Lohmann, G., Ionita, M. et al. (2022), AMOC modes linked with distinct North Atlantic deep water formation sites. *Climate Dynamics*, *59*, 837–849. doi:10.1007/s00382-022-06156-w

Döscher, R., Acosta, M., Alessandri, A., et al. (2022), The EC-Earth3 Earth system model for the Coupled Model Intercomparison Project 6. *Geoscientific Model Development*, *15*, 2973–3020. doi:10.5194/gmd-15-2973-2022

Friedrich, T., Timmermann, A., Menviel, L., et al. (2010), The mechanism behind internally generated centennial-to-millennial scale climate variability in an earth system model of intermediate complexity. *Geoscientific Model Development*, *3*, 377–389. doi: 10.5194/gmd-3-377-2010

Hawkins, E., & Sutton, R. (2007), Variability of the Atlantic thermohaline circulation described by three-dimensional empirical orthogonal functions. *Climate Dynamics*, *29*(7–8), 745–762. doi:10.1007/s00382-007-0263-8

Jackson, L., & Vellinga, M. (2013), Multidecadal to centennial variability of the AMOC: HadCM3 and a perturbed physics ensemble. *Journal of Climate*, *26*(7), 2390–2407. doi:10.1175/JCLI-D-11-00601.1

Jahn, A., & Holland, M. M. (2013), Implications of Arctic sea ice changes for North Atlantic deep convection and the meridional overturning circulation in CCSM4-CMIP5 simulations. *Geophysical Research Letters*, *40*, 1206–1211. doi:10.1002/grl.50183

Jiang, W., Gastineau, G., & Codron, F. (2021), Multicentennial variability driven by salinity exchanges between the Atlantic and the arctic ocean in a coupled climate model. *Journal of Advances in Modeling Earth Systems*, *13*(3), e2020MS002366. doi: 10.1029/2020MS002366

Jones, P. D., Briffa, K.R., Osborn, T.J., et al. (2009), High-resolution palaeoclimatology of the last millennium: A review of current status and future prospects. *Holocene*, *19*(1), 3–49. doi:10.1177/0959683608098952

Jungclaus, J. H., Haak, H., Latif, M., et al. (2005), Arctic-North Atlantic interactions and multidecadal variability of the meridional overturning circulation. *Journal of Climate*, *18*(19), 4013–4031. doi:10.1175/JCLI3462.1

Kilbourne, K.H., Wanamaker, A.D., Moffa-Sanchez, P. et al. (2022), Atlantic circulation change still uncertain. *Nature Geoscience*, *15*, 165–167. doi:10.1038/s41561-022-00896-4

Latif, M., Sun, J., Visbeck, M. et al. (2022), Natural variability has dominated Atlantic Meridional Overturning Circulation since 1900. *Nature Climate Chang*, *12*, 455–460. doi:10.1038/s41558-022-01342-4

Lapointe, F. , Bradley, R. S., Francus P., et al. (2020), Annually resolved Atlantic sea surface temperature variability over the past 2900y. *Proceedings of the National Academy of*

Sciences of the United States of America, *117*(44), 27171–27178. doi: 10.1073/pnas.2014166117.

Li, Y., & Yang, H. (2022), A Theory for Self-Sustained Multi-Centennial Oscillation of the Atlantic Meridional Overturning Circulation. *Journal of Climate*, *35*(18), 5883–5896. doi:10.1175/JCLI-D-21-0685.1

Mann, M. E., Zhang, Z., Rutherford, S., et al. (2009), Global signatures and dynamical origins of the Little Ice Age and Medieval Climate Anomaly. *Science*, *326*(5957), 1256–1260. doi:10.1126/science.1177303

Mann, M. E., Steinman, B. A., & Miller, S.K. (2014), On forced temperature changes, internal variability and the AMO. *Geophysical Research Letters*, *41*(9), 3211–3219. doi: 10.1002/2014GL059233

Mann, M. E., Steinman, B. A., Brouillette, D. J., et al. (2021), Multidecadal climate oscillations during the past millennium driven by volcanic forcing. *Science*, *371*(6533), 1014–1019. doi: 10.1126/science.abc5810

Meccia, V.L., Fuentes-Franco, R., Davini, P. et al. (2022), Internal multi-centennial variability of the Atlantic Meridional Overturning Circulation simulated by EC-Earth3. *Climate Dynamics*, doi:10.1007/s00382-022-06534-4.

Menary, M. B., Park, W., Lohmann, K., et al. (2012), A multimodel comparison of centennial Atlantic meridional overturning circulation variability. *Climate Dynamics*, *38*, 2377–2388. doi:10.1007/s00382-011-1172-4

Myriokefalitakis, S., Bergas-Massó, E., Gonçalves-Ageitos, M., et al. (2022), Multiphase processes in the EC-Earth model and their relevance to the atmospheric oxalate, sulfate, and iron cycles. *Geoscientific Model Development, 15*(7), 3079-3120. doi:10.5194/gmd-15-3079-2022

Ottera, O. H., Bentsen, M., Drange, H., et al. (2010), External forcing as a metronome for Atlantic multidecadal variability. *Nature Geoscience*, *3*, 688–694. doi: 10.1038/ngeo955

Pardaens, A., Vellinga, M., Wu, P., et al. (2008), Large-Scale Atlantic salinity changes over the last half-century: A model-observation comparison. *Journal of Climate*, *21*(8), 1698–1720. doi:10.1175/2007JCLI1988.1

Park, W., & Latif, M. (2008), Multidecadal and multicentennial variability of the meridional overturning circulation. *Geophysical Research Letters*, *35*(22), L22703. doi: 10.1029/2008GL035779

Rahmstorf S., Box, J. E., Feulner, G., et al. (2015), Exceptional twentieth-century slowdown in Atlantic Ocean overturning circulation. *Nature climate change*, *5*(5): 475–480. doi:10.1038/nclimate2554

Semedo, A., Soares, P. M., Lima, D. C., et al. (2016), The impact of climate change on the global coastal low-level wind jets: EC-EARTH simulations. *Global and Planetary Change, 137*, 88-106. doi:10.1016/j.gloplacha.2015.12.012

Sicre, M. A., Ezat, U., Guimbaut, E., et al. (2008), A 4500-year reconstruction of sea surface temperature variability at decadal time-scales off North Iceland. *Quaternary Science Reviews*, *27*(21-22), 2041–2047. doi:10.1016/j.quascirev.2008.08.009

Srokosz, M. A., & Bryden, H. L. (2015), Observing the Atlantic Meridional Overturning Circulation yields a decade of inevitable surprises. *Science*, *348*(6241), 1255575. doi: 10.1126/science.1255575

Thirumalai, K., Quinn, T. M., Okumura, Y., et al. (2018), Pronounced centennial-scale Atlantic Ocean climate variability correlated with Western Hemisphere hydroclimate. *Nature Communications*, *9*, 392. doi: 10.1038/s41467-018-02846-4

Vellinga, M., & Wu, P. (2004), Low-Latitude Freshwater Influence on Centennial Variability of the Atlantic Thermohaline Circulation. *Journal of Climate*, *17*(23), 4498–4511. doi: 10.1175/3219.1

Wyser, K., Kjellström, E., Koenigk, T., et al. (2020a), Warmer climate projections in EC-Earth3-Veg: The role of changes in the greenhouse gas concentrations from CMIP5 to CMIP6. *Environmental Research Letters, 15*(5), 054020. doi:10.1088/1748-9326/ab81c2

Wyser, K., van Noije, T., Yang, S., et al. (2020b), On the increased climate sensitivity in the EC-Earth model from CMIP5 to CMIP6. *Geoscientific Model Development, 13*(8), 3465-3474. doi:10.5194/gmd-13-3465-2020

Zhang, R., Sutton, R., Danabasoglu, G., et al. (2019), A review of the role of the Atlantic Meridional Overturning Circulation in Atlantic Multidecadal Variability and associated climate impacts. *Reviews of Geophysics*, *57*(2), 316–375. doi: 10.1029/2019RG000644

Zhang, Q., Berntell, E., Li, Q., et al. (2021), Understanding the variability of the rainfall dipole in West Africa using the EC-Earth last millennium simulation. *Climate Dynamics, 57*(1), 93-107. doi:10.1007/s00382-021-05696-x

Zhang, Q., Cao, N., & Power, K. E. (2022). Simulations for pre-industrial climate using EC-Earth3-LR model — selected data for a study on AMOC (Version 2) [Data set]. Zenodo. https://doi.org/10.5281/zenodo.7304486